

## Seismic response estimation of steel plate shear walls using nonlinear static methods

Moon Moon Dhar<sup>a</sup> and Anjan K. Bhowmick\*

*Department of Building, Civil and Environmental Engineering, Concordia University, Montreal, Canada*

*(Received October 09, 2015, Revised December 08, 2015, Accepted December 09, 2015)*

**Abstract.** One of the major components for performance based seismic design is accurate estimation of critical seismic demand parameters. While nonlinear seismic analysis is the most appropriate analysis method for estimation of seismic demand parameters, this method is very time consuming and complex. Single mode pushover analysis method, N2 method and multi-mode pushover analysis method, modal pushover analysis (MPA) are two nonlinear static methods that have recently been used for seismic performance evaluation of few lateral load-resisting systems. This paper further investigates the applicability of N2 and MPA methods for estimating the seismic demands of ductile unstiffened steel plate shear walls (SPSWs). Three different unstiffened SPSWs (4-, 8-, and 15-storey) designed according to capacity design approach were analysed under artificial and real ground motions for Vancouver. A comparison of seismic response quantities such as, height-wise distribution of floor displacements, storey drifts estimated using N2 and MPA methods with more accurate nonlinear seismic analysis indicates that both N2 and MPA procedures can reasonably estimate the peak top displacements for low-rise SPSW buildings. In addition, MPA procedure provides better predictions of inter-storey drifts for taller SPSW. The MPA procedure has been extended to provide better estimate of base shear of SPSW.

**Keywords:** nonlinear seismic analysis; N2 method; modal pushover analysis; finite element analysis

### 1. Introduction

Steel Plate Shear Walls (SPSWs) is an effective seismic load resisting system. A SPSW is made of a steel plate which is connected as an infill to the boundary beams and columns. Beams-to-columns connections may be either moment or simple connections. The steel infill plate is either welded or bolted to these boundary framing members using fishplates. In SPSWs, the thin infill plates are the main energy dissipation fuses which are allowed to buckle out-of-plane. The shear is primarily resisted by the diagonal tension field that forms in the thin infill plates when they buckle. Various experimental (Timler and Kulak 1983, Driver *et al.* 1998, Lubell *et al.* 2000, Behbahanifard *et al.* 2003, Guo *et al.* 2011, Sabouri-Ghomi and Sajjadi 2012) and analytical (Thorburn *et al.* 1983, Berman and Bruneau 2008, Bhowmick *et al.* 2008, Topkaya and Kurban 2009, Topkaya and Atasoy 2009, Qu and Bruneau 2010, Bhowmick *et al.* 2011) studies have been conducted on SPSWs and it is now known that SPSWs have large ductility with stable hysteretic

---

\*Corresponding author, Ph.D., E-mail: [anjan.bhowmick@concordia.ca](mailto:anjan.bhowmick@concordia.ca)

<sup>a</sup>M.A.Sc., E-mail: [moonmunni1990@gmail.com](mailto:moonmunni1990@gmail.com)

behaviors, great initial stiffness, and significant post buckling strength. Current Canadian (CAN/CSA-S16-09) and American (AISC 2010) steel design standards requires that SPSWs be designed according to capacity design approach. As per capacity design approach, for SPSWs, yielding in the steel infill plates and plastic hinging at the ends of beams are considered as the ductile fuses to dissipate seismic energy. The basic objective of the current code design approach including the capacity design approach is life safety for the design level earthquake while maintaining the serviceability after small frequent earthquakes. However, the actual reliability of the code design method in achieving these objectives is unknown. Recent earthquakes have shown that buildings may suffer irreparable or too costly to repair damages even during smaller earthquakes. Performance-based seismic design (PBSD) method which has emerged as a promising and efficient seismic design approach over the last decade provides engineers with the capability to design buildings that have a predictable and reliable performance during an earthquake. Accurate estimation of seismic demand parameters is the essential requirement for performance based seismic design. Seismic demands are best estimated using nonlinear time-history (NTH) analysis. But, this type of analysis requires a set of carefully selected spectrum compatible ground motion records. Additional computational effort and inherent complexity of NTH analyses make them not so popular in engineering design offices. Thus, simplified nonlinear static methods are adopted in various codes (CEN Eurocode 8; NBC 2010). These methods are based on monotonically increasing predefined load patterns until some target displacement is achieved. It is observed that simplified nonlinear static methods, known as pushover analysis, provide accurate seismic demand estimates only for low- to medium-rise moment frame buildings where the contributions of higher modes' response are not that significant (Nguyen *et al.* 2010). In order to overcome the drawbacks of conventional pushover analysis, a number of improved static procedures considering different loading vectors (derived from mode shapes) to account for higher mode effects were proposed. Among them the mostly used procedure is modal pushover analysis (MPA proposed by Chopra and Goel 2001). The fundamental assumption of MPA is that the coupling of structural responses due to different modes is neglected after the structure enters the inelastic stage. Such an assumption in MPA procedure simplifies estimation of structural responses of inelastic systems. MPA has been shown to increase the accuracy of seismic demand estimation in taller moment-frame buildings compared to the conventional pushover analysis (Chopra *et al.* 2004). In MPA procedure, pushover analysis is performed to determine maximum response of the structure due to its *n*th-vibration mode. Thus, concept wise MPA procedure does not increase any complexity as higher modes pushover analyses are similar to conventional first mode pushover analysis. Also, it was observed that MPA procedure considering the first few (two or three) modes contributions are usually sufficient (Chintanapakdee and Chopra 2003). However, the assumption of decoupling of structural responses in MPA might cause some estimation errors when compared with results from nonlinear time history analysis. Thus the procedure needs to be evaluated for any primary lateral load resisting system before use. The accuracy of this method has previously been studied on moment resisting frames (Chintanapakdee and Chopra 2003, Chopra and Goel 2001). Kalkan and Kunnath (2007) examined the performance of MPA procedure in estimating seismic demands of a set of existing steel and reinforced concrete buildings. Recently, Nguyen *et al.* (2010) investigates the applicability of MPA procedure for buckling-restrained braced frame (BRBF) buildings. Currently, there is no research available on application of MPA on SPSWs. SPSWs are increasingly used in medium to high rise buildings and such system exhibits different deformation characteristics from the frame structures. It is therefore necessary to extend the current research activity to evaluate the MPA for steel plate shear wall structures. This paper evaluates the

performance of modal pushover analysis of a low-rise (4-storey), medium rise (8-storey) and a high-rise (15-storey) SPSW. The analysis results are compared to the more accurate seismic analysis results from nonlinear dynamic time-history analysis.

Another nonlinear static method which is recommended in Eurocode 8 (CEN 2004) for performance evaluation and design verification of new and existing buildings is N2 method. The N2 method proposed by Fajfar (1999) is an easy to use nonlinear static method using constant ductility inelastic response spectrum. In this method, the seismic capacity curve is obtained from pushover analysis and the demand curve is represented by the design response spectrum. The intersection of the demand and capacity curve is called performance point, which provides visual representation of the probable performance of the structure for a particular seismic demand. Application of N2 method on the framed structures has been shown good predictions of seismic performance (Fajfar 1999). To date no research work has been conducted to assess the applicability of N2 method for estimating seismic demands of SPSWs. In this paper the accuracy of N2 method in estimating seismic performance parameters of SPSWs is studied by comparing results from N2 method with the accurate results of rigorous nonlinear dynamic analysis. The selected SPSWs (4-, 8-, and 15-storey SPSWs) have been designed in accordance with the NBCC 2010 and CAN/CSA S16-09 requirements and are analyzed for ground motions compatible with Vancouver, Canada.

## 2. Seismic design of steel plate shear wall system

A 4-storey and an 8-storey building with SPSWs were designed based on current capacity design approach of CSA/CAN S16-09 with an identical floor plan, which represents a hypothetical office building located in Vancouver. Total floor area of the buildings was 2631.7 m<sup>2</sup>. The building had two identical SPSWs in each direction to resist lateral forces, so each shear wall was designed to resist one-half of the design seismic loads. SPSWs were placed in such ways that maintained structural symmetry in both N-S and E-W directions. Therefore, only accidental torsion was considered in the equivalent static force calculation. The building was assumed to be on very dense soil and soft rock (soil class C according to NBCC 2010). The aspect ratio of SPSW was 1.5 with width of each shear wall panel as 5.7 m and height as 3.8m. A dead load of 4.26 kPa was used for each floor and 1.12 kPa for the roof. The live load on all floors was taken as 2.4 kPa. Snow loads applied at the roof were calculated following the provisions of NBCC 2010. The NBCC 2010 load combination  $D + 0.5L + E$  (where  $D$  = dead loads,  $L$  = live loads, and  $E$  = earthquake loads) was considered for intermediate floors and for the roof, the load combination  $D + 0.25S + E$  (where  $S$  = snow loads) was considered. Beam-to-column connections were considered as moment-resisting connections. In addition, the infill plates were connected with its boundary beams and columns with welded connections. Stiffness of the columns, top beam and bottom beam were designed to satisfy the requirements that are specified in CAN/CSA S16-09 to allow uniform tension field development in the adjacent infill plates. Boundary column design was performed according to capacity design approach of Berman and Bruneau (2008). The nominal yield strength of the boundary beams, columns and infill plates was assumed to be 350 MPa and all steel members were assumed to have a modulus of elasticity of 200,000 MPa. An infill plate thickness of 3.0 mm was assumed to be the minimum practical available plate thickness based on handling and welding considerations. Tables 1 and 2 present details of 4-storey and 8-storey SPSWs. The 15-storey SPSW was taken from Bhowmick *et al.* (2008). The width of 15-storey SPSW was 7.6 m

Table 1 Summary of 4-storey SPSW properties

4-storey SPSW			
Storey	Column sections	Beam sections	Plate
base		W690×240	
1-3	W360×463	W530×109	3
4	W360×463	W690×240	3

Table 2 Summary of 8-storey SPSW properties

8-storey SPSW			
Storey	Column sections	Beam sections	Plate
base		W690×350	
1-2	W360×634	W530×109	4.8
3	W360×382	W530×109	4.8
4	W360×382	W690×192	4.8
5-7	W360×216	W530×109	3
8	W360×216	W690×350	3

Table 3 Summary of 15-storey SPSW properties

15-storey SPSW			
Storey	Column sections	Beam sections	Plate
base			
1-3	W360×990	W410×100	3
4-6	W360×900	W410×100	3
7-9	W360×744	W410×100	3
10-12	W360×634	W410×100	3
13-14	W360×592	W410×100	3
15	W360×592	W760×582	3

(aspect ratio of 2.0) and total height of the 15-storey SPSW was 57 m from the ground. The 15-storey SPSW was designed according to indirect capacity design approach specified in ANSI/AISC 341-10. Details of the 15-storey SPSW design are described in Bhowmick *et al.* (2008). Table 3 presents details of 15-storey SPSW.

### 3. Nonlinear finite element model

The selected SPSWs were modelled and analyzed using ABAQUS Standard. Beams, columns, and infill plates were modelled using general purpose four node doubly curved shell elements with reduced integration (ABAQUS element S4R). The element S4R accounts for finite membrane strains and large rotations. This element has six degrees of freedom per node: three translations and three rotations. In FEM, steel plates were directly connected with its boundary elements, and

thus fishplates were ignored. Fabrication error, welding distortion and deformation of boundary beam due to gravity load cause initial imperfection in infill plate. In this study, initial imperfection pattern was considered corresponding to the first buckling mode shape as loaded in the physical test. The out of plane deformation was considered as two times of the corresponding plate thickness. The finite element modeling technique was validated with a quasi-static cyclic test result of a 4-storey SPSW specimen tested by Driver *et al.* (1998). Driver *et al.* (1998) tested a four storey SPSW under quasi-static cyclic loading. The geometry of the 4-storey SPSW, along with the finite element mesh, is shown in Fig. 1. Details of the test including the material properties are available in the literature (Driver *et al.* 1998). Hysteresis curves obtained from the finite element analysis were compared with the test results in Fig. 2. An excellent agreement was observed between finite element analysis and experimental results. Both the capacity and the stiffness of the SPSW were predicted well. The hysteresis curves generated by the analysis show slightly less pinching than observed during the test.

For seismic analysis a dummy gravity column was incorporated into the finite element model to account of  $P-\Delta$  effects. The dummy column is connected to the plate wall at every floor level with pin ended rigid links, which maintains the constant horizontal displacement between SPSW and gravity column. This gravity column was made of 2-node linear 3-D truss (ABAQUS T2D3) and was designed to carry half of the total remaining mass at each floor level. The gravity loads of each storey were added as lumped masses on the columns at corresponding floor. A bilinear elasto-plastic stress-strain curve was adopted for steel beams, columns, and infill plates. A Rayleigh damping model was used with 5% critical damping ratios for the first two modes of vibration, which include a cumulative modal mass equal to more than 90% of the total mass applied on the SPSW.

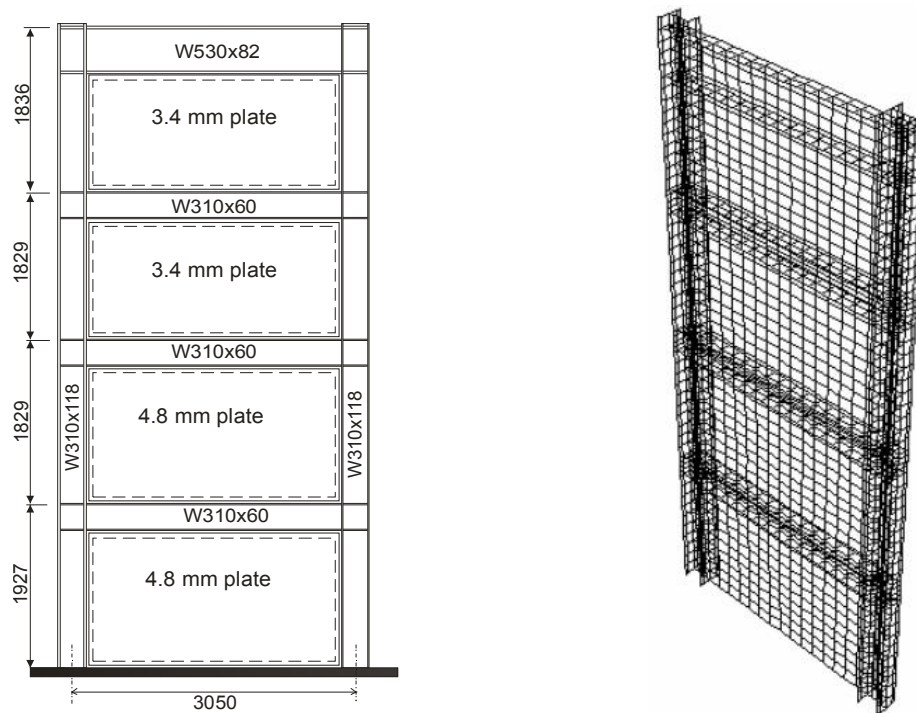


Fig. 1 Test specimen of Driver *et al.* (1998) and FE mesh

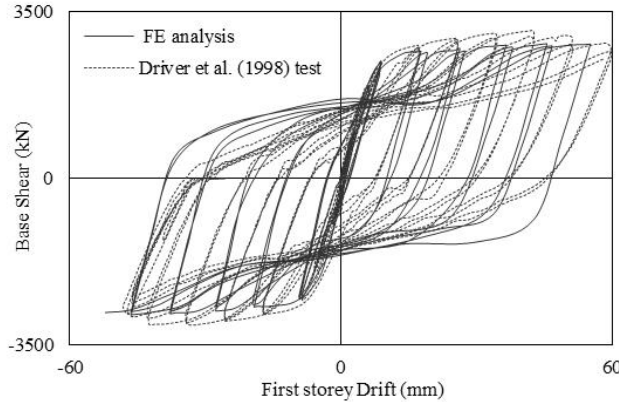


Fig. 2 Validation of cyclic curves for Driver *et al.* (1998) SPSW test

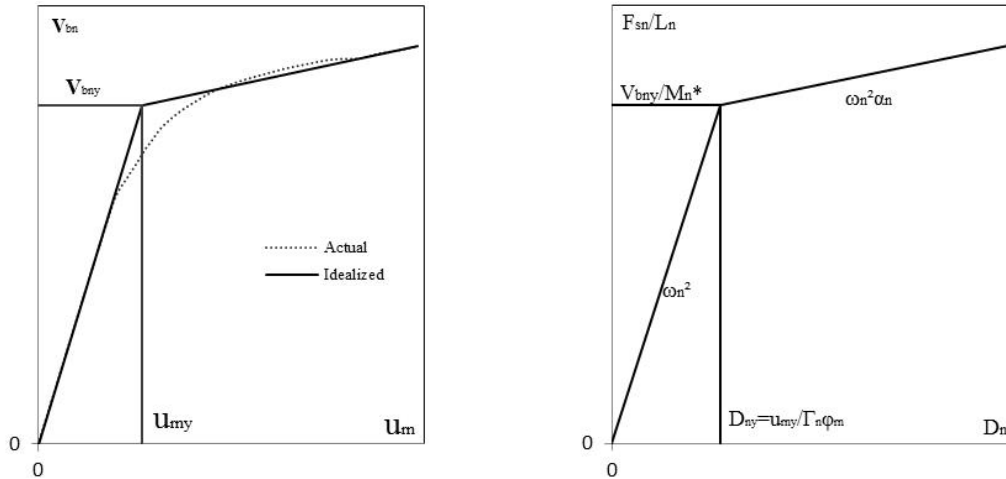


Fig. 3 Schematic figure of actual pushover curve and idealized pushover curve (left) and  $F_{sn}/L_n$ - $D_n$  relation (right) (Chopra and Goel 2001)

#### 4. Review of selected nonlinear static procedures

A brief review of Modal pushover analysis (MPA), N2 method and NBC 2010 lateral load pattern is presented in this section. This will be followed by the application of these three methods in estimating seismic demands of the selected SPSWs.

##### 4.1 NBCC 2010 lateral load pattern

According to the NBCC 2010, the lateral force at any story,  $F_x$ , is calculated from the following formula

$$F_x = (V - F_t) \frac{W_x h_x}{\sum_{i=1}^{i=n} W_i h_i} \tag{1}$$

where  $F_t$  is an extra lateral force component applicable to the top floor;  $V$  is design seismic base shear;  $W_i$  or  $W_x$  denotes the dead load in addition to 25% snow load applicable to the storey  $i$  or  $x$  and  $h_x$  or  $h_i$  denotes the height from the base to the storey level  $i$  or  $x$  respectively.

The design seismic base shear ( $V$ ) can be calculated as follows

$$V = \frac{S(T_d)M_V I_E W}{R_d R_0} \geq \frac{S(2.0)M_V I_E W}{R_d R_0} \quad (2)$$

where  $S(T_d)$  is the spectral acceleration;  $M_V$  is an amplification factor accounting for higher mode effects on base shear;  $I_E$  is the importance factor for the structure;  $W$  denotes the total dead load in addition to 25% of the snow load;  $R_d$  denotes the force modification factor of the structure related to ductility;  $R_0$  denotes the over-strength related force modification factor of the structure. The values of  $R_d$  and  $R_0$  are provided in NBCC 2010 and CSA S16-09 as 5.0 and 1.6 respectively.

According to the NBCC 2010, for structures having  $R_d$  greater than 1.5 the design base shear should assume a maximum value as

$$V \leq \frac{2S(0.2)I_E W}{3R_d R_0} \quad (3)$$

#### 4.2 Modal pushover analysis

In MPA procedure, pushover analysis is performed to determine maximum response of the structure due to its  $n^{\text{th}}$  vibration mode. Lateral force distribution pattern in the MPA is associated with its inertia force for different mode of vibration. Base shear-roof displacement curve of the MDOF system is idealized as a bilinear force-deformation relation of the  $n^{\text{th}}$ -mode inelastic SDOF system. The SPSW is pushed up to the peak deformation of the  $n^{\text{th}}$ -mode inelastic SDOF system which is determined by nonlinear dynamic analysis of that SDOF system. Any appropriate modal combination rule may apply to combine all peak modal responses. A step-by-step summary of the MPA procedure to estimate the seismic demands for SPSW building is presented here:

- Step-01: Estimate the natural frequencies of the SPSW,  $\omega_n$ , and associated normalized mode shape vectors,  $\phi_n$ , for linearly elastic vibration modes of the SPSW.
- Step-02: Compute the base shear-roof-displacement ( $V_{bn}-u_{rn}$ ) pushover curve for lateral force distribution of  $S_n^* = m_i \phi_{in}$  for  $n^{\text{th}}$ -mode of the SPSW ( $m_i$  is the mass of  $i^{\text{th}}$ -storey). During the pushover analysis this force distribution is assumed to be constant. Physical basis of this force distribution is the inertial force of the structure that opposes the deformation due to the external forces.
- Step-03: Convert the regular pushover curves of each “mode” into bilinear idealized curves according FEMA 273 (FEMA 1997).
- Step-04:  $V_{bn}-u_{rn}$  pushover curves are then converted into force-displacement relation ( $F_{sn}/L_n-D_n$ ) of  $n^{\text{th}}$ -mode inelastic SDOF system using following two relations of force and displacement.

$$F_{sn} = \frac{V_{bn}}{\Gamma_n} \quad \text{where} \quad \Gamma_n = \frac{\phi_n^T m \mathbf{1}}{\phi_n^T m \phi_n} \quad (4)$$

$$D_n = \frac{u_{rn}}{\Gamma_n \phi_{rn}} \quad L_n = \phi_n^T m \iota \quad (5)$$

where  $\Gamma_n$  is modal participation factor, each element of the influence vector  $\iota$  is equal to unity and  $L_n$  is the mass of SDOF system. Schematic diagram of actual and idealized pushover curves are shown in Fig. 3.

Step-05: Compute the peak deformation of the  $n^{\text{th}}$ -mode inelastic SDOF system  $D_n$ , by solving the following equation or from inelastic response spectrum.

$$\ddot{D}_n + 2\xi_n \omega_n \dot{D}_n + \frac{F_{sn}}{L_n} = -\ddot{u}_g(t) \quad (6)$$

where  $\xi_n$  is the damping ratio of  $n^{\text{th}}$ -mode for inelastic SDOF system.

Step-06: Calculate the peak deformation of MDOF system,  $u_{rn}$ , using the relation:  $u(t) = \Gamma_n \phi_n D_n(t)$ . Other parameters such as floor displacement, inter-storey drift can also be calculated in the same way. Finally, total responses of the structure are calculated by combining results of all the effective modes.

#### 4.3 N2 method

As proposed by Fajfar (1999) the N2 method integrates the conventional pushover analysis with an inelastic response spectrum. Pushover curve which represents the capacity of the structure is converted into equivalent spectral accelerations and spectral displacement by using effective modal mass and modal participation factors. Response spectrum is used as the seismic demands of the structure. After that, both curves are plotted in the same coordinate from which demand-capacity relationship is obtained. The steps of N2 method are as follows:

##### Development of seismic demand curve

Seismic demand is usually defined as the elastic (pseudo)-acceleration spectrum where spectral accelerations ( $S_{ae}$ ) are given as a function of the natural period of the structure  $T$ . Site specific design spectrum can be used to develop a seismic demand curve. The first step for developing a seismic demand curve is to convert a traditional response spectrum in acceleration – displacement format.

##### Seismic Demand in Acceleration Displacement Response Spectrum Format (ADRS)

Acceleration response spectrum can be converted into acceleration-displacement response spectrum (ADRS) by utilizing the following relation between Pseudo-acceleration and displacement for the Single-Degree-of-Freedom (SDOF) system

$$S_{de} = \frac{T^2}{4\pi^2} S_{ae} \quad (7)$$

where  $S_{de}$  and  $S_{ae}$  are the spectral displacement and pseudo acceleration of elastic response spectrum respectively corresponding to the period  $T$  and for a fixed viscous damping ratio.

Inelastic ADRS can be obtained indirectly from elastic ADRS by using strength reduction

factor  $R_\mu$  proposed by Vidic *et al.* (1994). As given in Eq. (8), force reduction factor ( $R_\mu$ ) is the ratio of elastic strength demand to inelastic strength demand of an SDOF system for a specified ductility ratio

$$S_a = \frac{S_{ae}}{R_\mu} \tag{8}$$

From Eqs. (7) and (8)

$$S_d = \mu \frac{T}{4\pi^2} S_a \tag{9}$$

where  $\mu$  is the ductility factor defined as the ratio between the maximum displacement and the yield displacement.

Several studies (Miranda and Bertero 1994, Vidic *et al.* 1994) have been conducted to determine force reduction factor. In this research, the formulae proposed by Vidic *et al.* (1994) in slightly modified form will be used.

$$R_\mu = (\mu - 1) \frac{T}{T_o} + 1 \quad \text{when } T \leq T_o \tag{10}$$

$$R_\mu = \mu \quad \text{when } T \geq T_o \tag{11}$$

$$T_o = 0.65 \mu^{0.3} T_c \leq T_c \tag{12}$$

where  $T_c$  is the characteristics period which refers the transition period where constant acceleration region intersect the constant velocity region and this is the period when largest forces are applied to the structure;  $T_o$  is the transition period which depends on structural ductility and it should not be greater than  $T_c$ .

The values of characteristics period and the transition period can be considered equal. Thus, in the simple version of the N2 method, Fajfar (1999) considered

$$T_o = T_c \tag{13}$$

Once the ductility and force reduction factors are known, constant ductility seismic demand spectrum can be obtained for different ductility.

**Development of capacity curve of Equivalent-Single Degree of Freedom (ESDOF) system**

Step-1: Pushover curve of MDOF system: Base shear-roof displacement relation (pushover curve) for MDOF system is developed by pushing the structure with lateral force proportional to the assumed displacement shape ( $\phi_i$ ) multiplied by storey mass,  $m_i$ .

$$p_i = m_i \phi_i \tag{14}$$

where  $p_i$  is the lateral force at any storey  $i$ .

Step-2: Determination of Capacity Spectrum for ESDOF system: The MDOF system is

transformed into ESDOF system. Top displacement ( $D_t$ ) and base shear ( $V_b$ ) of MDOF system are transformed into force ( $F^*$ )-displacement ( $D_t^*$ ) relationship of ESDOF system by the following relationship.

$$F^* = V_b / \Gamma \quad D_t^* = D_t / \Gamma \quad (15)$$

where  $\Gamma$  is called modal participation factor as defined in Eq. (4).

Step-3: Idealize the pushover curve of ESDOF into an elastic-perfectly plastic form following the guidelines provided in FEMA-273. Finally, bilinear idealized force ( $F^*$ )-displacement ( $D_t^*$ ) curve is transferred into capacity curve by representing spectral acceleration to spectral displacement curve of ESDOF system.

#### Determination of seismic demand and performance of ESDOF system

Demand spectra and capacity spectra for SDOF system are drawn in the same plot. Intersection point of the radial line of the capacity curve corresponding to the elastic stiffness of the SDOF system and the elastic demand spectrum gives the elastic strength requirement ( $S_{ae}$ ) of the structure. The yield acceleration ( $S_{ay}$ ) for the SDOF system refers the acceleration requirements for the inelastic behavior. Ratio of the elastic acceleration demand and inelastic acceleration capacity is the reduction factor  $R_{\mu}$ . After that, ductility can be calculated by the reverse calculation of Eqs. (10) and (11).

### 5. Selected earthquake ground motion records

ASCE 7-10 recommends minimum three ground motion records for response history analysis, when peak responses are considered to investigate seismic response of structure. Moreover, minimum seven ground motion records are suggested for the same purpose when average of maximum responses is used. Four real ground motion records and four simulated (artificial) records are selected for this study. The real ground motions are collected from strong ground motion database of Pacific Earthquake Engineering Research center, California (PEER 2010). Real Ground Motion Records (GMR) were selected as such that they have peak ground acceleration (A) to peak ground velocity (V) ratio close to 1.0, which is the recommended value for Vancouver region (Naumoski *et al.* 2004). Only horizontal components of the ground motion records were selected for this study. The simulated GMRs are collected from engineering Seismotoolbox (Atkinson 2009). They were chosen for site class C with the magnitude of 6.5 and 7.5. Table 4 and Table 5 present some important features of the four real ground motion records and four simulated earthquake records.

The selected ground motions were scaled based on the partial area method (Naumoski *et al.* 2004) of ground motion scaling. According to this method, the area under the acceleration response spectrum curve of the selected ground motion and design response spectrum are compared and made equal by finding out a suitable scaling factor. Area under the acceleration response spectrum of selected GMRs ( $A_2$ ) between  $0.2T_1$  to  $1.5T_1$  ( $T_1$  is the first period of vibration of the building) has been compared with the area under the design response spectrum of Vancouver ( $A_1$ ) for the same period range. Scaling factor for selected GMR is the ratio of  $A_1/A_2$  where both of the response spectrums are obtained for 5% of critically damped single degree of freedom system. Scaling factors for all the selected earthquakes were calculated and are provided in Table 4 and Table 5.

Table 4 Ground motion parameters of selected real ground motions

Event name	Magnitude	PGA (g)	A/V	Scaling factor 4-storey	Scaling factor 8-storey	Scaling factor 15-storey
San Fernando, California, 1971	6.6	0.188	1.04	1.63	1.58	1.06
Kobe, Japan, 1995	6.6	0.143	0.97	1.71	1.56	1.47
Kern Country, California, 1952	6.53	0.156	1.02	1.89	1.81	1.53
Imperial Valley, California, 1979	6.53	0.525	1.04	0.996	1.03	0.614

Table 5 Parameters of selected simulated earthquake records

Event name	Magnitude	Scaling factor 4-storey	Scaling factor 8-storey	Scaling factor 15-storey
6C1	6.5	0.696	0.78	0.82
6C2	6.5	1.303	1.48	1.32
7C1	7.5	0.815	0.91	0.694
7C2	7.5	1.629	1.83	1.28

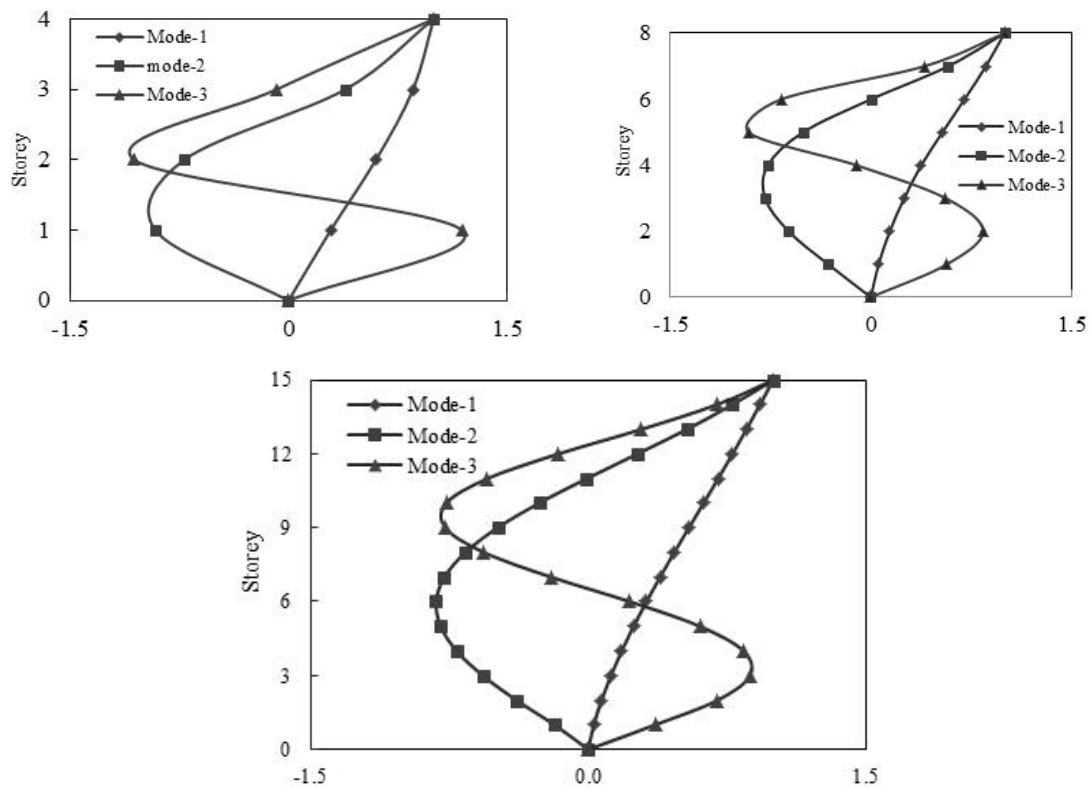


Fig. 4 Mode shapes of 4, 8, and 15 storey SPSWs

## 6. Application of MPA and N2 method on SPSW

Frequency analyses were performed for all SPSWs to calculate elastic vibration periods and the corresponding modes. In Fig. 4, first three elastic mode shapes of selected SPSWs are presented. Lateral forces calculated from inertia forces and proportional to mode shapes were applied incrementally. Gravity loads were applied prior to pushover analysis. Fig. 5 presents the base shear-roof displacement curve for first three-modes of selected SPSWs. 1<sup>st</sup> “mode” pushover curve of all SPSWs were similar to the regular pushover curves, where the structure displaced in the same direction as its original yield mechanism.

Roof displacements after yielding, 2<sup>nd</sup> “mode” pushover curve of all SPSWs, were opposite to their original mechanism due to the local column plastic hinge formation. This type of pushover

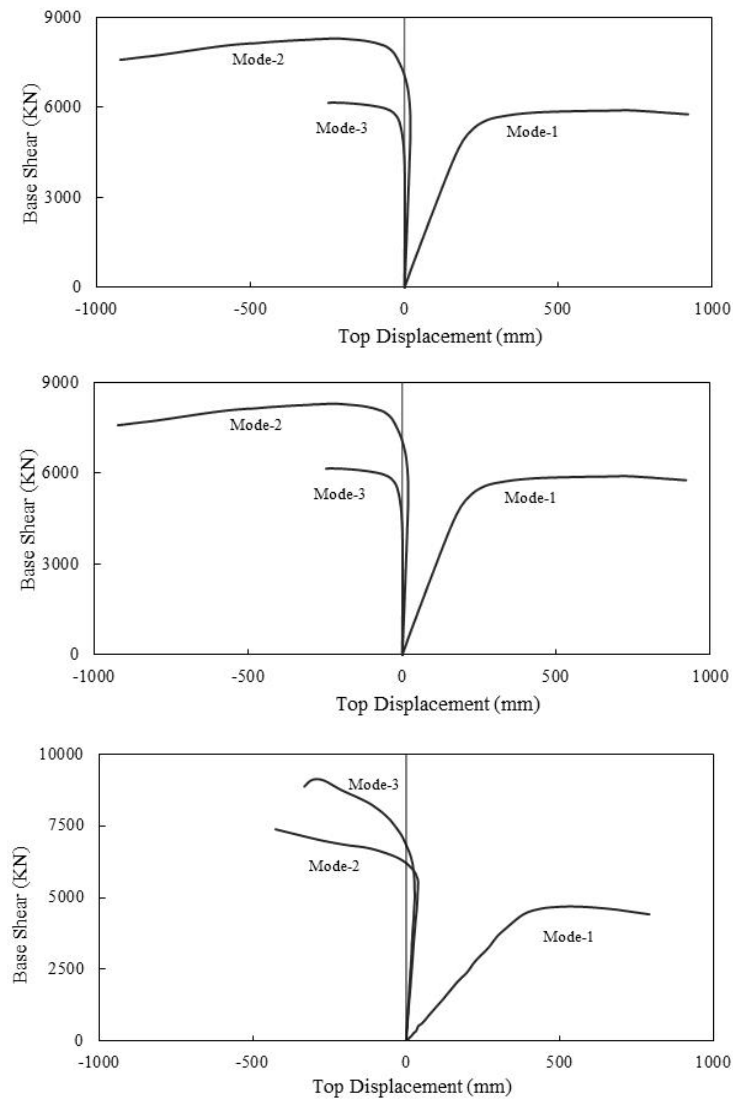


Fig. 5 Modal pushover curves for 4-storey (top), 8-storey (middle) and 15-storey (bottom) SPSWs

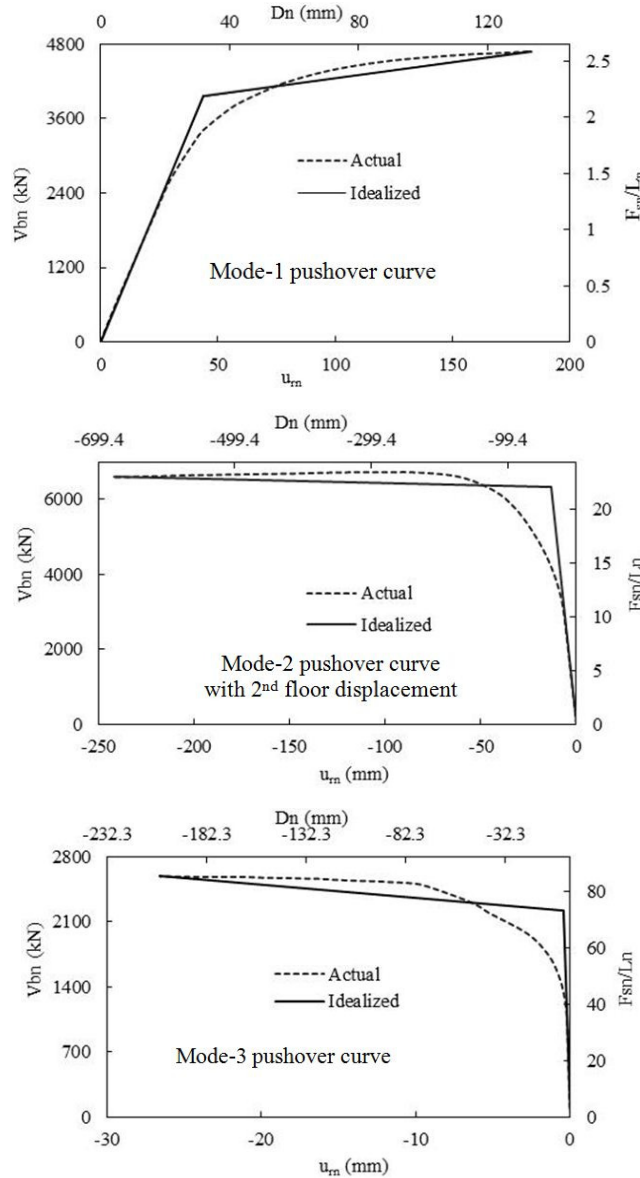


Fig. 6 Actual, idealized pushover curves of MDOF ( $V_{bn}-u_m$ ) and SDOF systems ( $F_{sn}/L_n-D_n$ ) for 4-storey SPSW

curve pattern is often called “reversal” in pushover. "Reversal" in the pushover curve arises when a local mechanism forms and roof moves opposite to its original mechanism due to the resultant storey force. For 15-storey SPSW, 3<sup>rd</sup> mode pushover curve was also “reversed” pushover curve. According to Goel and Chopra (2005), “reversal” in pushover can be avoided by plotting base shear against the displacement of a different floor above the yielded stories of the building. The resulting pushover curve can then be used in the MPA procedure. This approach was adopted for all the cases where reversal was observed. For instance, for the 4-storey SPSW, local plastic

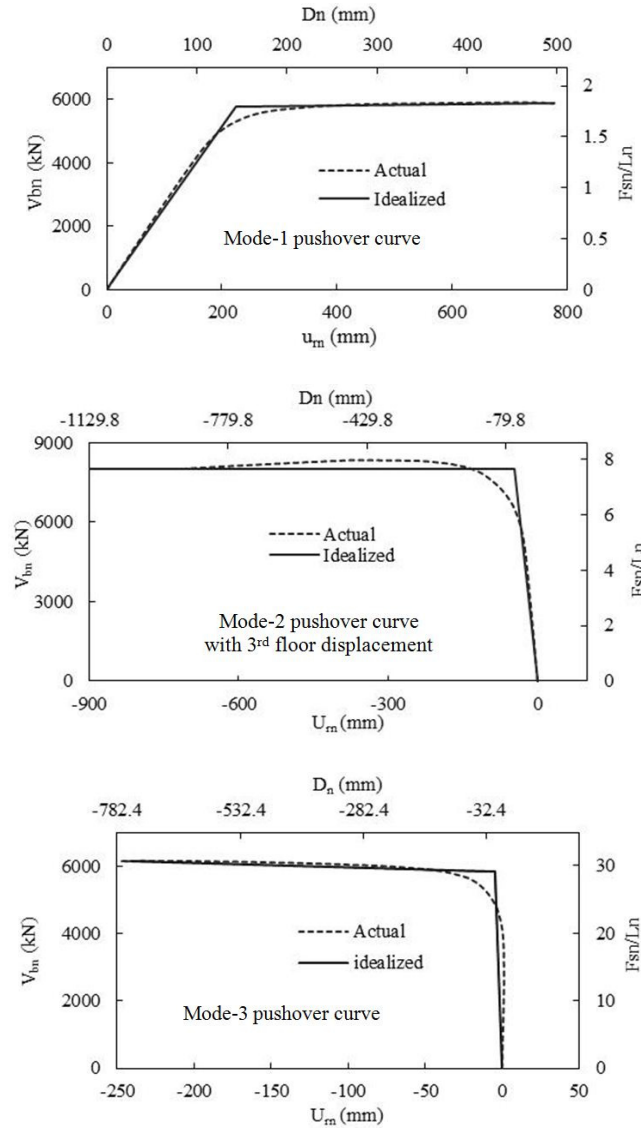


Fig. 7 Actual, idealized pushover curves of MDOF ( $V_{bn}-u_{rn}$ ) and SDOF systems ( $F_{sn}/L_n-D_n$ ) for 8-storey SPSW

mechanism formed at the first floor during the “2nd-mode” pushover analysis. Therefore, pushover curve for base-shear versus 2<sup>nd</sup> storey displacement, which was a “regular” pushover curve, was used for MPA procedure. All pushover curves of the selected SPSWs were idealized into bilinear curves. Base shear-roof displacement ( $V_{bn}-u_{rn}$ ) pushover curves of MDOF were converted into force-displacement relation ( $F_{sn}/L_n-D_n$ ) of n<sup>th</sup>-mode inelastic SDOF. Initial slope of the curve is the initial stiffness and second slope is the post yielding stiffness. Actual pushover curve and idealized pushover curve for MDOF and SDOF are presented in the same plot in Figs. 6, 7, and 8.

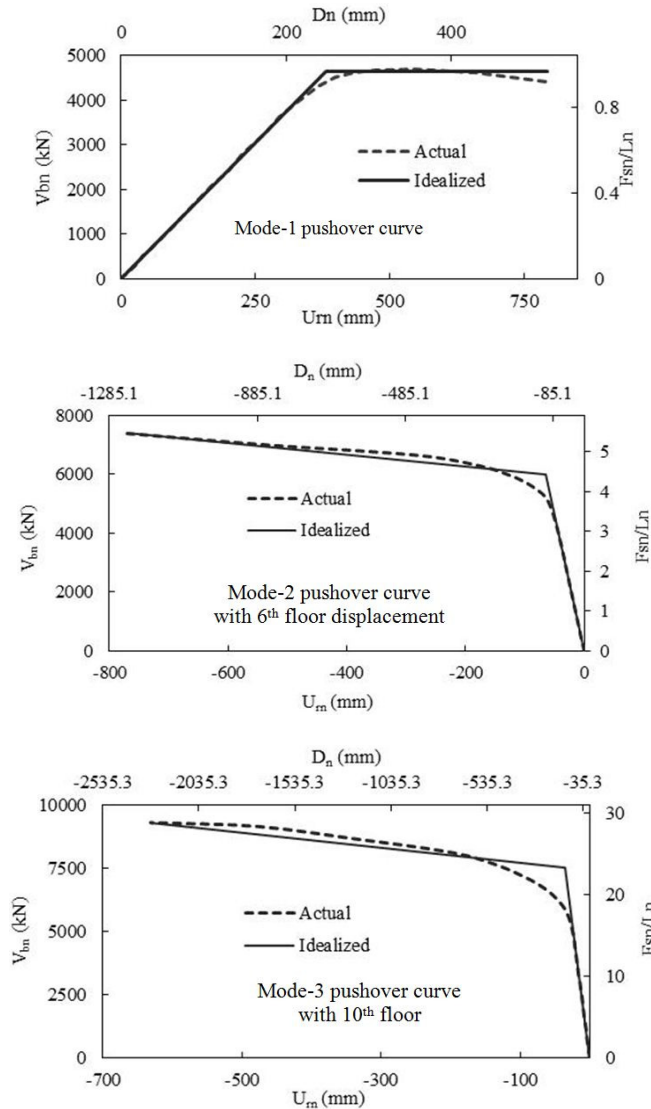


Fig. 8 Actual, idealized pushover curves of MDOF ( $V_{bn}-u_{mn}$ ) and SDOF systems ( $F_{sn}/L_n-D_n$ ) for 15-storey SPSW

Calculated peak deformations of SDOF systems,  $D_n$ , were utilized to calculate the peak deformation of MDOF ( $u_{rno}$ ). Then, other properties such as floor displacements and inter-storey drifts were also calculated from the  $u_{rno}$ . Modal combination rule SRSS has been utilized to combine the modal responses. Maximum displacements, inter-storey drifts were estimated for 1-mode, 2-modes and 3-modes combination.

For N2 method, bilinear idealized force-displacement curves associated with 1<sup>st</sup> mode were converted into spectral acceleration versus spectral displacement curves of SDOF systems for all three selected SPSWs. These are known as capacity curves and are presented in Figs. 9, 10, and 11. Vancouver design response spectrum (5% damped) was used to obtain seismic demand curve. For

inelastic SDOF system, acceleration spectrum,  $S_a$ , and displacement spectrum,  $S_d$ , were determined from elastic ADRS by using reduction factor obtained from Eqs. (10) and (11). In the beginning of this procedure, demand curve was constructed for elastic response of the structure (e.g., ductility factor is equal to one). Demand spectra and capacity spectra for SDOF system were drawn in the same plot. Figs. 9, 10, and 11 present graphical representation of capacity curve of SDOF

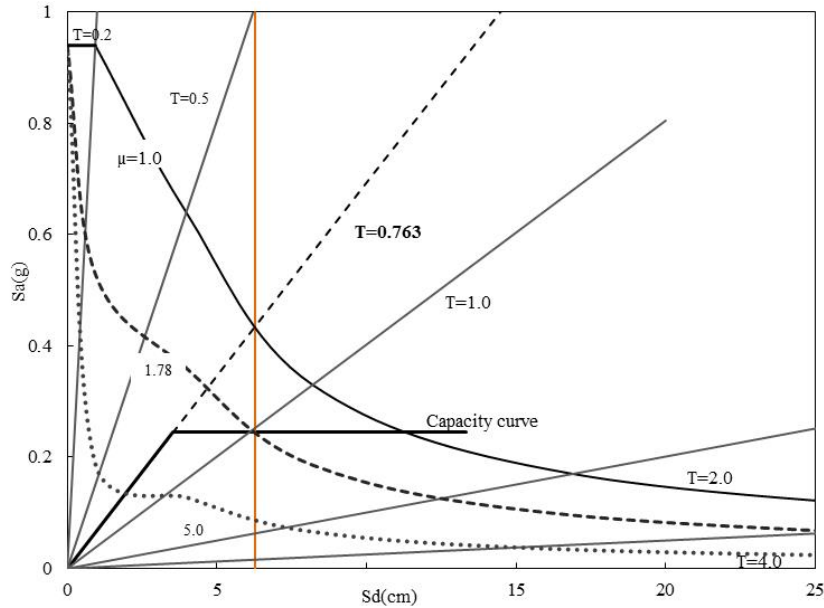


Fig. 9 Demand and capacity spectra for 4-Storey SPSW

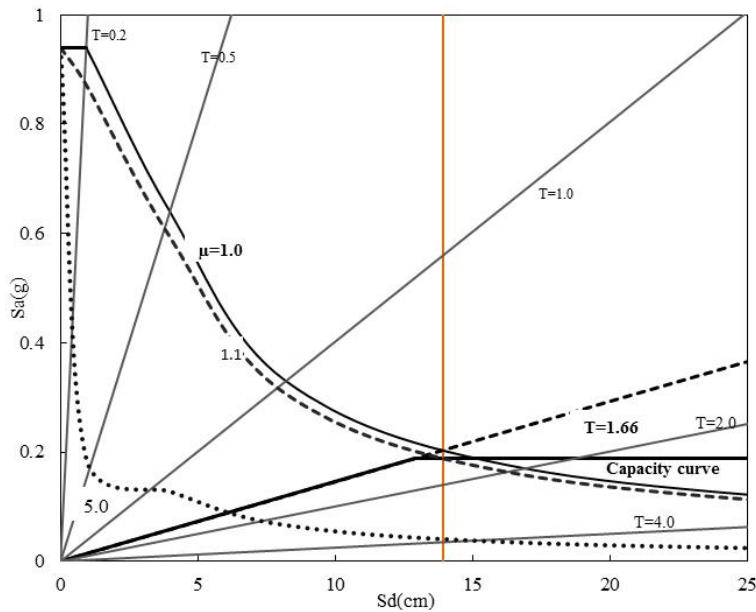


Fig. 10 Demand and capacity spectra for 8-Storey SPSW

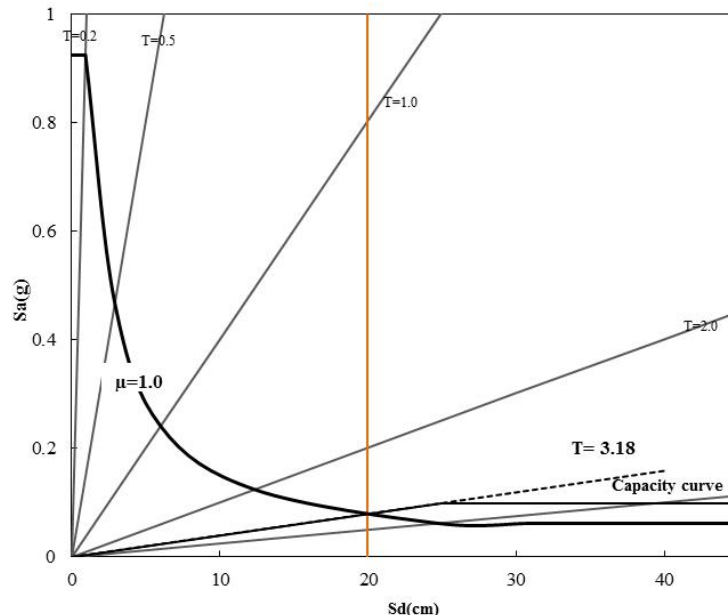


Fig. 11 Demand and capacity spectra for 15-Storey SPSW

system of 4-storey, 8-storey and 15-storey SPSW system. For 4-storey and 8-storey SPSW systems, elastic demand spectrum was generated from Vancouver design response spectrum for soil class C. On the other hand, elastic demand spectrum for 15-storey SPSW was estimated from Vancouver design response spectrum for soil class B. This was because the 15-storey SPSW studied was designed for soil class B. Displacement demands were determined from the intersection points of the capacity curves and the demand curves corresponding to the ductility demands. Finally, displacement demands of SDOF systems were transferred into displacement demand of MDOF by reverse transformation. In this study, top displacement demands for 4-storey and 8-storey SPSW buildings were 85.97 mm and 217.64 mm respectively. These values are very close to the values obtained from nonlinear time history analysis. For 15-storey SPSW, as presented in Fig. 11, the capacity curve intersected the demand curve of ductility one, meaning that the 15-storey SPSW remained elastic for the design earthquake. The displacement demand of 15-storey SPSW was estimated from the intersection point, which was 305.53 mm. Table 6 compares between the maximum top displacements of the selected SPSWs by N2 method and nonlinear time history analysis.

According to NBC 2010, ductility based reduction factor for SPSW is 5.0. Ductility demands obtained from N2 method for 4- and 8- storey SPSWs were lower than the code suggested ductility. This was because of use of thicker than required infill plate thickness to maintain practical availability and handling requirements. Moreover, framing action in beams and columns had a significant contribution to the storey shear resistance. Thus, overall capacities of the SPSWs were very high, which was one of the major reasons for lower ductility demands. A seismic demand spectrum for ductility factor of 5.0 was also presented for 4- and 8-storey SPSWs in Figs. 9 and 10.

Estimated results from MPA and N2 method are compared, in Figs. 12, 13, and 14, with results obtained from nonlinear-seismic analysis and regular pushover analysis using NBCC 2010 lateral load pattern. Fig. 12 shows that for low rise SPSW, NLTHA displacement pattern did not closely

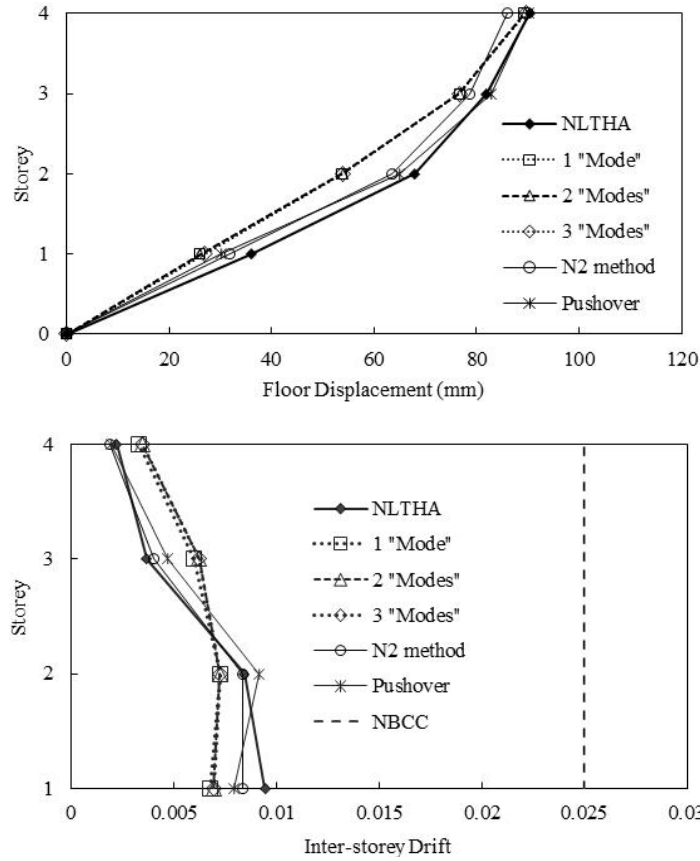


Fig. 12 Height wise variation of floor displacements and inter-storey drifts of 4-storey SPSW from NLTHA, MPA, N2 method, and regular pushover analysis

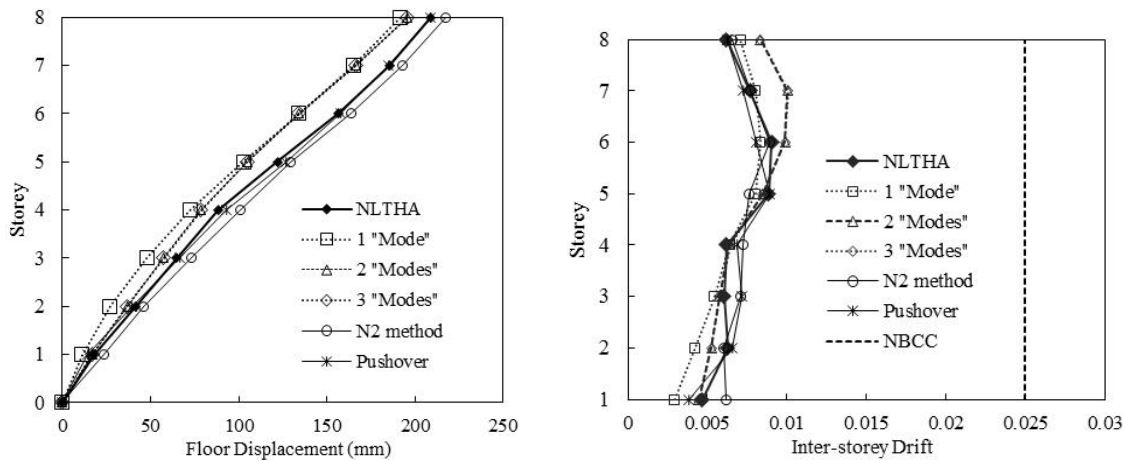


Fig. 13 Height wise variation of floor displacements and inter-storey drifts of 8-storey SPSW from NLTHA, MPA, N2 method, and regular pushover analysis

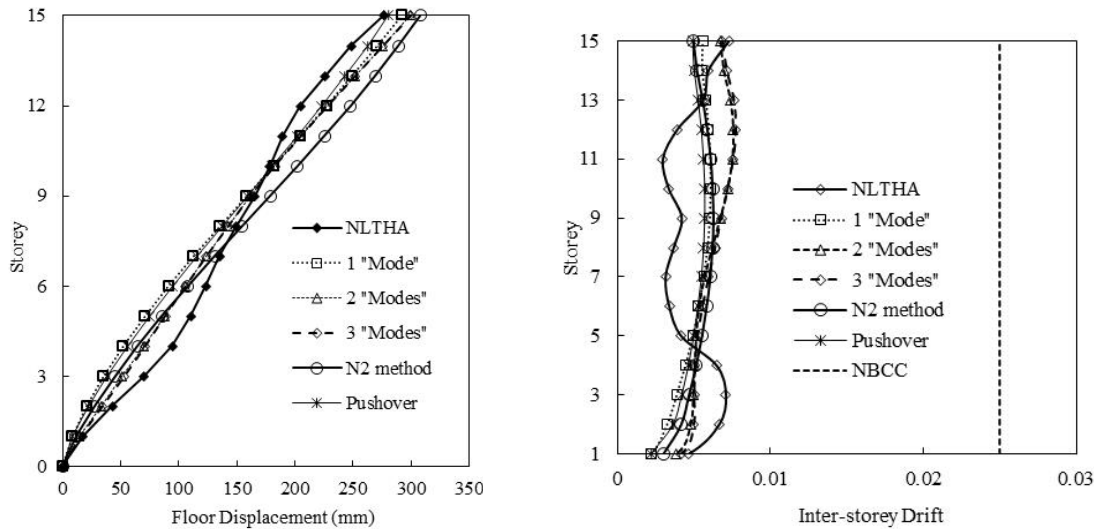


Fig. 14 Height wise variation of floor displacements and inter-storey drifts of 15-storey SPSW from NLTHA, MPA, N2 method, and regular pushover analysis

follow its mode shape pattern. In comparison to MPA, regular pushover analysis following NBC 2010 equivalent lateral load pattern was able to reasonably predict the floor displacements. However, inter-storey drifts were underestimated in the bottom storeys but overestimated at the top.

For medium-rise SPSW (8-storey SPSW), Fig. 13 shows that, 1-mode combination did not predict floor displacements and inter-storey drifts very well and 2-mode combination significantly improved the predictions at the bottom floors. However, 3<sup>rd</sup>-mode contribution did not make any difference to displacements and inter-storey drifts for medium-rise SPSW. It was also observed that regular pushover analysis using NBC 2010 load pattern reasonably predicted the floor displacements of mid-rise SPSW. However, inter-storey drifts were underestimated by regular pushover analysis at the upper storeys.

MPA for high-rise SPSW, as presented in Fig. 14, showed considerable higher mode contribution. 2-mode combination improved the predictions of displacements. Once 3<sup>rd</sup> mode contribution was added, it significantly improved displacements and inter-storey drifts at the lower storeys. It was also observed that in comparison to MPA, regular pushover analysis significantly underestimated displacements and inter-storey drifts at the lower storeys. It was also observed

Table 6 Performance of the selected SPSWs using N2 method

Parameters	4-Storey building	8-Storey building	15-Storey building
Ductility (Pushover)	4.8	2.6	2.3
Ductility (N2 method)	1.78	1.11	N/A
Maximum top displacement (mm)-N2 method	85.97	217.64	305.53
Maximum average top displacement(mm)-NLTHA	92.61	208.84	276.3
Error in top displacement demand	7.17%	4.21%	10.58%

Table 7 Base shear from different methods

SPSW	Base shear (kN)				
	MPA	Modified MPA	N2 method	NLTHA	Pushover
4- storey	5224	3950	4261	4273	4510
8- storey	9586	6271	5217	6615	5480
15- storey	6771	5302	3762	5822	2893

from Figs. 12, 13, and 14 that storey displacement demands of low-rise SPSW buildings (4- and 8-storey) can be predicted accurately by N2 method. However, inter-storey drifts for 8-storey and 15-storey were not predicted well by N2 method.

Finally, base shears for all the selected SPSWs were obtained from N2 method and MPA method and compared with seismic analysis results. Table 7 shows that N2 method can closely predict the base shear for low-rise SPSW, such as for 4-storey SPSW. However, for 8- and 15-storey SPSWs, N2 method significantly underestimated the base shears. One important observation from Table 7 is that MPA significantly overestimates the base shears in SPSWs and thus modification is required in MPA procedure to better estimate base shear of SPSW. One such modification is proposed in this research. Though the main energy dissipating element in SPSW is the steel infill plate, it was observed in previous research (Bhowmick *et al.* 2008) that more than 25% of the total shear is resisted by the boundary framing members at the base. Also, for all the selected SPSWs in this study, seismic analysis showed that about 30% of the total shear was resisted by the boundary columns. Canadian seismic provision, CAN/CSA S16-09 also requires that boundary frame of SPSW must have the flexural strength to resist at least 25% of the total shear force. For this proposed modification to MPA procedure to estimate base shear, it is assumed that boundary members will resist about  $\beta\%$  of the total shear and the rest of the shear will be resisted by the infill plate at the base. One can approximately estimate the contribution of the boundary columns ( $\beta$ ) in resisting the base shear from elastic analysis or first mode pushover analysis of SPSW. The capacity of an infill plate,  $V_n$ , of SPSW in shear is given by

$$V_n = 0.5F_y wL \sin 2\alpha \quad (16)$$

where  $F_y$  is the yield strength of the infill plate;  $w$  is the infill plate thickness;  $L$  is infill plate width;  $\alpha$  is the angle of the tension field developed in the infill plate and is obtained from CAN/CSA-S16-09.

Since the maximum shear in the infill plate is limited by the capacity of the infill plate, it is possible to calculate the maximum base shear ( $V$ ) of SPSW by equating  $(1 - \beta)V$  to  $V_n$ . Thus, according to the proposed modification, the maximum value of base shear by MPA procedure is

$$\frac{V_n}{(1 - \beta)}$$

and are presented in Table 7. For the selected SPSWs, first mode pushover analysis showed that about 30% of the total shear was resisted by the boundary framing members. Thus, for this study, 30% shear contribution by boundary members was assumed for all cases. It was observed from Table 7 that with the proposed modifications, MPA predicted the base shears for SPSWs very well.

## 7. Conclusions

This paper evaluates the effectiveness of commonly used nonlinear static procedures in predicting seismic demands of regular ductile steel plate shear wall buildings. The key findings from this study are as follows:

- (1) The finite element model developed in this study was able to provide reasonably accurate predictions of the behaviour of SPSW. Excellent agreement was observed between results from FE analysis and results from quasi-static cyclic test.
- (2) Modal pushover analysis showed that local storey mechanisms, which could not be detected by the traditional pushover analysis with code specified equivalent lateral loads or using first mode of vibration, developed for higher modes of vibration. However, seismic analysis did not show any local mechanism for the selected SPSWs.
- (3) The accuracy of the MPA in predicting the floor displacements and storey-drift ratios of SPSWs was improved by including the first two modes in the procedure relative to using only the fundamental mode. However, using first three modes did not improve the accuracy of the peak floor displacement noticeably, but there was little improvement in the estimation of storey-drift ratios. Thus, the second mode contribution was higher in comparison to the higher modes contributions in the responses.
- (4) Excellent accuracy of N2 method was noticed for low-rise SPSW in terms of top displacement demand and ductility demand. The disagreement between nonlinear seismic analysis and N2 method increased with an increase in building height. This was because, for high-rise SPSW, contributions from higher modes were not considered in the N2 method.
- (5) It was observed from this comparative study that regular pushover analysis using NBC 2010 load pattern reasonably predicted the floor displacements of low-to-mid-rise SPSWs. However, inter-storey drifts were not predicted well by regular pushover analysis.
- (6) The proposed modification in the MPA procedure was able to provide better estimates of base shears for the selected SPSWs.

## Acknowledgments

Funding for this research project is provided by the Faculty of Engineering and Computer Science, Concordia University, Montreal, Canada and the Natural Sciences and Engineering Research Council of Canada. The authors also gratefully acknowledge Professor Rakesh K. Goel at the California Polytechnic State University, San Luis Obispo for his valuable help with the MPA procedure.

## References

- ANSI/AISC (2010), *Seismic Provisions for Structural Steel Buildings*; American Institute of Steel Construction Inc., Chicago, IL, USA.
- Applied Technology Council (1996), *Seismic Evaluation and Retrofit of Concrete Buildings*; ATC-40, Seismic Safety Commission, State of California, CA, USA.
- ASCE (2010), *Minimum Design Loads for Buildings and other Structures*; American Society of Civil Engineers, VA, USA.

- Atkinson, G.M. (2009), Earthquake Time Histories Compatible with the 2005 NBCC Uniform Hazard Spectrum. URL: [www.seismotoolbox.ca](http://www.seismotoolbox.ca)
- Behbahanifard, M., Gilbert, R., Grondin, Y. and Elwi, A.E. (2003), "Experimental and numerical investigation of steel plate shear walls", Department of Civil and Environmental Engineering, University of Alberta; Edmonton, Canada.
- Berman, J.W. and Bruneau, M. (2008), "Capacity design of vertical boundary elements in steel plate shear walls", *Eng. J.*, **45**(1), 57-71.
- Bhowmick, A.K., Driver, R.G. and Grondin, G.Y. (2008), "Nonlinear seismic analysis of steel plate shear walls considering strain rate and P-delta effects", *J. Construct. Steel Res.*, **65**(5), 1149-1159.
- Bhowmick, A.K., Grondin, G.Y. and Driver, R.G. (2011), "Estimating fundamental periods of steel plate shear walls", *Eng. Struct.*, **33**(6), 1883-1893.
- CEN. Eurocode 8 (2001), Design of Structures for Earthquake Resistance, Part – 1; European Standard prEN 1998-1, Draft No. 4, European Committee for Standardization, Brussels, Belgium.
- Chintanapakdee, C. and Chopra, A.K. (2003), "Evaluation of modal pushover analysis using generic frames", *Earthq. Eng. Struct. Dyn.*, **32**(3), 417-442.
- Chopra, A.K. and Goel, R.K. (2001), "A modal pushover analysis procedure to estimate seismic demands for buildings: Theory and preliminary evaluation", Pacific Earthquake Engineering Research Center; CA, USA.
- Chopra, A.K., Goel, R.K. and Chintanapakdee, C. (2004), "Evaluation of a modified MPA procedure assuming higher modes as elastic to estimate seismic demands", *Earthq. Spectra*, **20**(3), 757-778.
- CSA (2009), "Limit states design of steel structures", Canadian Standards Association, Toronto, ON, Canada.
- Driver, R.G., Kulak, G.L., Kennedy, D.J.L. and Elwi, A.E. (1998), "Cyclic test of four storey steel plate shear wall", *J. Struct. Eng., ASCE*, **124**(2), 112-120.
- Fajfar, P. (1999), "Capacity spectrum method based on inelastic demand spectra", *Earthq. Eng. Struct. Dyn.*, **28**(9), 979-993.
- FEMA (1997), NEHRP Guidelines for the Seismic Rehabilitation of Buildings; FEMA-273, Applied Technology Council for the Building Seismic Safety Council, Washington, D.C., USA.
- FEMA (2005), Improvement of Nonlinear Static Seismic Analysis Procedures: FEMA-440, Applied Technology Council (ATC-55 Project), Washington, D.C., USA.
- Goel, R.K. and Chopra, A.K. (2005), "Role of higher-Mode" pushover analysis in seismic analysis of the buildings", *Earthq. Spectra*, **21**(5), 1027-1041.
- Guo, L., Rong, Q., Ma, X. and Zhang, S. (2011), "Behavior of steel plate shear wall connected to frame beams only", *Int. J. Steel Struct.*, **11**(4), 467-479.
- John, A. and Halchuk, S. (2003), "Fourth generation seismic hazard maps of Canada: Values for over 650 Canadian localities intended for the 2005 national building code of Canada", Geological Survey of Canada, Ottawa, ON, Canada.
- Kalkan, E. and Kunnath, S.K. (2007), "Assessment of current nonlinear static procedures for seismic evaluation of buildings", *Eng. Struct.*, **29**(3), 305-316.
- Lubell, A.S., Prion, H.G.L., Ventura C.E. and Rezai, M. (2000), "Unstiffened steel plate shear wall performance under cyclic load", *J. Struct. Eng., ASCE*, **126**(4), 453-460.
- Miranda, E. and Bertero, V.V. (1994), "Evaluation of strength reduction factors for earthquake resistant design", *Earthq. Spectra*, **10**(2), 357-379.
- Naumoski, N., Murat S. and Kambiz, A.H. (2004), "Effects of scaling of earthquake excitations on the dynamic response of reinforced concrete frame buildings", *Proceedings of the 13th World Conference on Earthquake Engineering*, Vancouver, BC, Canada, August.
- NBCC (2010), National Building Code of Canada; Canadian Commission on Building and Fire Codes, National Research Council of Canada (NRCC), Ottawa, ON, Canada.
- Nguyen, A.H., Chintanapakdee, C. and Hayashikawa, T. (2010), "Assessment of current nonlinear static procedures for seismic evaluation of BRBF buildings", *J. Construct. Steel Res.*, **66**(8-9), 1118-1127.
- PEER (2010), Next Generation Attenuation of Ground Motions Project (NGA) Database; Pacific Earthquake

- Engineering Research Center, Berkely, CA, USA.
- Qu, B. and Bruneau, M. (2010), "Capacity design of intermediate horizontal boundary elements of steel plate shear walls", *J. Struct. Eng.*, **136** (6), 665-675.
- Sabouri-Ghomi, S. and Sajjadi, S.R.A. (2012), "Experimental and theoretical studies of steel shear walls with and without stiffeners", *J. Construct. Steel Res.*, **75**, 152-159.
- Thorburn, L.J., Kulak, G.L. and Montgomery, C.J. (1983), "Analysis of steel plate shear walls", Structural Report No. 107; Department of Civil and Environmental Engineering, University of Alberta, Edmonton, AB, Canada.
- Timler, P.A. and Kulak, G.L. (1983), "Experimental study of steel plate shear walls", Structural Engineering Report No. 114; Department of Civil Engineering, University of Alberta, Edmonton, AB, Canada.
- Topkaya, C. and Atasoy, M. (2009), "Lateral stiffness of steel plate shear wall systems", *Thin-Wall. Struct.*, **47**(8-9), 827-835.
- Topkaya, C. and Kurban, C.O. (2009), "Natural periods of steel plate shear wall systems", *J. Construct. Steel Res.*, **65**(3), 542-551.
- Vidic, T., Fajfar, P. and Fischinger, M. (1994), "Consistent inelastic design spectra: Strength and displacement", *Earthq. Eng. Struct. Dyn.*, **23**(5), 507-521.

DL